Study on the influence of F16 fault on rockburst

Hai Rong
Liaoning Technical University
Liting Pan
Liaoning Technical University
Yadi Wang (wangyadi18@163.com)
Liaoning Technical University
Shiqi Yu
Liaoning Technical University
Kaipeng Guo
Liaoning Technical University
Nannan Li
Liaoning Technical University

Article

Keywords: rock burst, F16 fault, Displacement monitoring, Tension monitoring

Posted Date: March 28th, 2022

DOI: https://doi.org/10.21203/rs.3.rs-1457160/v1

Abstract

In order to solve the safety problem of rockburst in coal mining under fault conditions and realize safe and efficient production of coal mine, this paper analyzes the existing mechanism and geological environment of fault, constructs fault monitoring scheme and field construction method, and carries out underground monitoring of F16 fault. The stress and displacement of F16 fault in Gengcun Coal Mine are monitored, the deformation and activity of the fault are analyzed, and the influence on energy when the stress and displacement change is observed. The experimental results show that : Before and after the two large energy microseismic events, the stress and displacement changed significantly, and the energy increased first and then decreased sharply. The mining of working face had an important impact on the activity of F16 fault. The deep mining of coal mine would disturb the coal seam and roof and floor strata, destroy the stress state of the original rock mass, increase the in-situ stress, complicate the geological structure, and develop various faults one after another, It will destroy the integrity and integrity of the coal seam, cause the destruction of surrounding rock near the fault, release energy, cause large energy microseismic events, and in serious cases, it will lead to rockburst accidents. The research results have guiding significance for monitoring the impact of F16 fault activity on Rockburst in Gengcun Coal Mine, and provide experimental methods and theoretical basis for other coal mines to study the change process of energy during fault activity.

1. Introduction

The stress value generally rises with the support pressure of the coal wall increases and the stress concentration coefficient increases, which can easily lead to large-scale rock mass destruction events near it. In severe cases, rock burst accidents will occur. On the other hand, there is no way to do that. The results of the study show that a rock burst is closely related to horizontal tectonic stress. If the tectonic stress and the mining stress are superimposed, the fault may appear activation or slip locally, but will impact the nearby coal and rock mass. Due to the cause of fault shock rock pressure, the possibility of fault shock rock pressure will gradually increase. [1,2]The fault rock burst is one of the major geological disasters.

The rock burst is caused by the coupling of geodynamic environment and mining engineering effects. The majority of the studies on rock burst are carried out from a perspective of mining engineering effects. There are no studies on my geodynamic conditions. In fact, power and energy sources of rock burst aren't limited to roadway or mining face. The range of rock mass involved in rock bursts is considerably bigger than the mining space scale. It's also necessary to further analyze the geodynamic force of rock bursting from the macro scale. The conditions need to be studied. Aiming at the risk prediction and prevention of the fault rock burst, Sun Yuzhen [3] analyzed the fault formation mechanism and roadway deformation factors, studied the basic characteristics of the fault and the mechanism of the rock burst, and concluded that the formation of the F16 fault is due to The superposition of stress and control the occurrence of rock burst in Yima mining area. Luo Hao et al. [4] studied the evolutionary law of surrounding rock stress field with the increase of mining depth and the process of approaching the F16 fault by combining

numerical calculation and similar material experiments. It shows that with the increase of the mining depth and the proximity of the F16 fault, the stress concentration degree of the surrounding rock increases, and the impact risk increases. Zhao Shankun et al. [5] studied the F16 faults from different angles by using theoretical analysis, numerical simulation and other methods. The results show that the fault is affected by the mining of the working face, which reduces the stability of the fault contact surface and the surrounding rock of the working face, and the energy of coal and rock mass accumulates. The stress increases, and under the influence of mining disturbance, rock bursts are prone to occur. Tian Fujun[6] established a comprehensive prevention and control system integrating various means such as safety training, monitoring and early warning, crisis relief measures, effect inspection, safety protection, etc. The mine pressure prevention and control has achieved good results. Kang Hongpu et al.[7] analyzed the influence of faults on the value and direction of in-situ stress, and found that the horizontal stress in some areas near the fault has decreased, and large faults will cause the direction of the maximum horizontal principal stress to reverse. On the basis of the measured data, the FLAC3D numerical calculation software was used to analyze the distribution of the in-situ stress field around the large-scale synclinal structure in the Huating mining area, and compared with the measured in-situ stress data. The in-situ stress measurement and numerical simulation are organically combined to fully understand the distribution characteristics of the underground in-situ stress field in coal mines. Zhang Yanbo et al. [8] conducted a numerical simulation study on the rock burst of the deep-buried roadway fault. The simulation results show that the closer the deep mining activities are to the fault, the greater the stress concentrated on the fault. As the stress continues to accumulate, when the ultimate strength of the coal body is reached, the accumulated elastic energy will be released through injection and other methods to induce the fault rock burst. Cao Minghui et al.[9] studied the influence of the width of the fault coal pillar on the activation instability of the fault and the energy change inside the fault coal pillar. The UDEC numerical simulation software was used to establish a plane strain model, and it was shown that when the fault coal pillar width decreases, the coal pillar supporting pressure The peak value increases, the elastic strain energy increases, and the fault appears to activate and release energy to the coal pillar. Jia Teng et al. [10] analyzed the evolution law of stress peak value and elastic strain energy near the fault under different conditions such as elastic modulus of coal seam, coal burial depth and roof lithology based on FLAC3D numerical simulation software. Dou Yunfeng et al.[11] used the finite element software ANSYS to simulate the impact of coal seam at the fault in order to effectively and accurately predict the risk of coal seam rock burst, and analyzed the influence of the fault on the size and distribution of coal rock stress. : The fault has a great influence on the stress distribution of coal and rock, that is, the stress gradient near the fault is large, and the stress concentration position of the coal rock mainly occurs near the intersection of the fault and the coal seam. Even if the coal seam near the fault has no impact tendency, the coal seam may exist Strong impact risk. Dai Linchao[12] summarized the achievements of the current fault rock burst in theoretical research, experimental research and numerical simulation research, which is helpful to deeply understand the mechanism of fault rock burst. Zeng Linsheng et al. [13] studied the mechanism of rock burst risk induced by fault activity under the influence of mining through numerical simulation, and concluded that the longer the advancing length of the working face and the larger the fault dip angle, the easier it is to cause rock burst. The properties also have an

important influence on the occurrence of rock bursts. Pan Yishan et al.[14] regarded the fault rock burst as the deformation and instability of the fault zone and the surrounding rock system of the upper and lower walls, established a criterion for determining the stability of the disturbance response, and analyzed a simple model of the fault rock burst. Over-stick-slip instability model, explaining the intermittency of fault rock burst. Wang Suna et al. [15] studied the coal control mode of the F16 fault and its influence on the occurrence of coal seams by using field geological survey and indoor comprehensive analysis, and analyzed the spatial location and distribution characteristics of the F16 fault and its occurrence in coal seams. Liu Jinhai et al.[16] proposed the viewpoint of dynamic and static bearing pressure of longwall stope to explain the rockburst phenomenon in the process of deep coal mining. Taking the F16 fault as an example, Li Zhonghua et al. [17] established a mechanical model of the influence of working face mining on the fault, and applied the theoretical calculation method to obtain the shortest distance between the coal wall and the fault when the fault is affected. Peng Suping et al.[18] analyzed the high-angle normal faults with different dips, the deformation and failure of the roof rock mass and the distribution of rock pressure under the influence of mining, and the "activation" of the fault zone and its influence range under the influence of mining. The rock mass inside is broken, and the periodic fault step is small, the caving zone is high, especially the footwall of the fault, and the roof stability is poor. Jiang Yaodong et al.[19,20] studied the mechanism and law of rock burst in coal mines, the deformation and failure law of deep intermittent coal and rock mass, the distribution of mining stress, and the temporal and spatial evolution characteristics of energy field. Dong Sensen et al. [21] used a high-precision microseismic monitoring system and a stress real-time online monitoring system to monitor the fault-pregnancy process of the longwall working face, and used a numerical simulation method to simulate the mining process, and the fault area obtained during the monitoring process was analyzed. The coupling analysis of activation information and the displacement field and stress field obtained by numerical simulation can quickly judge the activation law of rock and soil, and can give early warning of geological disasters such as rock burst and water inrush during mining. Luo Hao[22] used numerical calculation and similar material method to study the evolution law of surrounding rock stress field with the increase of mining depth and close to F16 fault, and concluded that with the increase of mining depth, the stress concentration degree of F16 fault surrounding rock became higher, Affected by the F16 fault and the coal pillar at the stope boundary, the rockburst occurrence mode is high stress and large-scale regional instability. Zhenhua Jiao[23] analyzed the correlation between the fault structure and the temporal and spatial characteristics of the rock burst by collecting the rock burst events that occurred near the fault during the deep mining process based on the engineering background of deep mining near the fault in the Yima coalfield. It is concluded that the rockburst risk is positively related to the mining depth, and negatively related to the distance to the F16 fault. The occurrence frequency and intensity of rockburst near the F16 fault increase significantly. Lei Wang[24] studied the mining stress evolution and reactivation characteristics of the F16 reverse fault during the withdrawal induction period of the Yima coalfield. Based on the 3D digital elevation model of the GIS platform, and using AutoCAD software to construct the fault, it was concluded that the footwall of the F16 fault is a high stress concentration area.. Affected by the F16 fault and the huge thick glutenite on the roof, a large amount of elastic strain energy is accumulated in the coal seam near the fault, which increases the possibility of rock burst damage

during the mining process. Hongwei Wang[25] used physical and numerical simulation methods to study the slip of reverse fault structure caused by coal mining in Yima mining area, Henan Province. The stress evolution around the fault is analyzed, and it is concluded that the normal stress of the fault surface is relatively larger than the shear stress, and the normal stress and shear stress of the fault surface close to the coal seam are larger than the normal stress and shear stress of the fault surface far away from the coal seam. Sheng Xue[26] simulated the fault movement process in the process of coal seam extraction by establishing a physical simulation model, and studied the precursory information of fault slip, using digital speckle image correlation method, shear stress sensor and acoustic emission monitoring in the simulation. By monitoring the fault displacement and shear stress, the evolution characteristics of the fault displacement and the fault slip position in the Yima mining area of Henan are finally obtained.

Regarding the relationship between high-energy microseismic events, rock bursts and fault activity, most of the previous studies were carried out from the qualitative aspect, and there were few reports on the quantitative research.

2 Geological Structure Background

2.1 working conditions of Geng Village

The Gengcun mine field is bounded by the 2–3 coal seam outcrop in the north; the F16 fault in the south; the Qianqiu Mine and the Yuejin Mine in the east by the 41 exploration line; the Yangcun Mine is adjacent by the F5101 fault in the west. The ore field is 4.5 km long from east to west; the north-south slope is 2.6 km wide, and the field area is about 11.503 km2.

Gengcun Coal Mine was put into operation in 1982 with a intended production capacity of 1.2 million tons per year. After several system upgrades and link transformations, the approved production capacity is 3.6 million tons/year. The mine implements the inclined vertical shaft to go up and down the mountain at a single level, adopts the long-wall mining method, the entirely mechanized mining top coal caving technology, and the roof management of all caving methods. The coal seam of the Yima Formation of the Middle Jurassic is mined in the mine. The main coal seam is 2–3 coal, the average dip angle of the coal seam is 10°, the thickness of the coal seam is 0.24–21.73 m, and the average thickness is 8.96 m. The 2–3 coal seam is a semi-dark coal type, and the coal seam hardness is f = 1.5. The coal seam is easilyto spontaneously combust, and has a weak impact tendency, and the coal dust has the danger of explosion.

2.2 F16 fault geological structure

The 16 fault is resulted by the enormous compressive stress from south to north caused by the activity of the Nanpingquan fault under the action of the Yanshan movement after the deposition of coal measures in the Yima Coalfield, causing the block between the F16 fault and the Nanpingquan fault to trend northward. Forming. The F16 thrust fault, the Kishi thrust fault in the west and the Nanpingquan thrust fault in the south together form a regional large-scale thrust-napped structural belt near EW. The

inclination angle of the section is generally between 20° and 70°. In the west of the Yima Coalfield, the F16 section has a single structure with a large inclination angle, and gradually becomes slower in the east, and the section structure is more complicated. The development of the F16 thrust fault caused the coal seam in the southern part of the Yima coalfield to undergo traction and inversion, and promoted rheological action in many coal seams. The spatial occurrence and thickness of the coal seam changed abnormally, as shown in Fig. 1.

Because the fault destroys the continuity of the coal layer, the evolutionary law of mining stress becomes very complicated. The existence of faults leads to discontinuity of coal strata. The mechanism of fault-type rock burst is also very complicated. In recent years, rockburst disaster accidents under the influence of faults have increased significantly. The rockburst caused by fault activation is extremely destructive due to the large volume of potential sources and the large released energy.

3. Analysis Of Influence Of F16 Fault On Rockburst

3.1 study on influence range of F16 fault on rockburst

Statistics on the distance between the 107 shock events that have occurred in the Yima mining area and the F16 fault, the area with a distance of more than 1000 m from the F16 fault has 8 shock events; Within the range of 500–1000 m, 48 shock events occurred; in the area less than 500 m, 51 shock events occurred. It is judged that the distance between shock events and the F16 fault is negatively correlated. Figure 2 shows the distribution of rockburst dangerous areas in the Yima coalfield.

The Yima mining area is affected by the F16 fault, which causes the coal and rock mass in the mining area to accumulate energy, and the stress gradually increases. The 13200 working face cutting hole intersects with the F16 fault, and the stop line is 236 m away from the fault. Under the influence of mining disturbances The activity of the F16 fault increases, and the belt adjacent to the F16 fault and the core of the Yima syncline are areas of tectonic stress concentration and high-risk areas of rock burst.

The influence range of the fault calculated by geodynamic zoning is shown in Eq. (1–1). When the straight line distance between the mine field boundary and the active fault is less than the influence range of the fault, it will have a certain influence on coal mining and rock burst occurrence.

$$b = K \cdot 10h \quad (1–1)$$

In the formula: k is the activity coefficient (k = 1, 2, 3), k = 3 when the fracture activity is strong, k = 2 when it is moderate, and k = 1 when it is weak; h is the vertical drop of the fracture, m.

F16 is a regional thrust fault with an extension length of about 24 km, strikes nearly east-west, dips slightly eastward from south, shallow dip is 75°, deep dip is generally 15–35°, and the drop is 50–500 m. When the F16 fault activity is When it is moderate, the range of the influence zone of the F16 fault is about: =2×10×50 ~ 2×10×500 = 1 km ~ 10 km.

The drop of the F16 fault near the 13th mining area of Gengcun Coal Mine is 350–380 m. According to the above formula, the width of the F16 fault influence zone is 7000–7600 m. It can be seen from this that the 13200 working face is all in the influence zone of the F16 fault. Under the influence of the F16 fault, the mining activities of the working face are easy to cause the dislocation and slip of the upper and lower walls of the fault, and it is easy to cause the damage of the surrounding coal and rock mass, and the accumulated elasticity It can be released to cause dynamic disasters such as rock bursts.

The above research shows that the F16 fault has an important influence on the occurrence of rock bursts in the Gengcun coal mine. The research should be compared with the actual activity data of the F16 fault to improve the reliability of the research results. Therefore, it is very necessary to carry out the monitoring of the F16 fault downhole and to understand the changes of the displacement and stress of the F16 fault during the production process.

3.2 study on generation energy of Rockburst of F16 fault

The occurrence of rock burst is the unity of time and space, so the analysis of the microseismic events monitored by the microseismic monitoring system should first focus on the location of the microseismic events and the energy of the microseismic events monitored by the microseismic monitoring system, especially for mines. "High-energy" microseismic events above the critical energy of rock burst, When a high-energy microseismic event occurs in a certain area, it indicates that the coal and rock mass has the "potential" for rock burst, and has the energy basis for rock burst. After that, there is a danger of high-energy microseismic events or even ground pressure shocks occurring again [31].

Figure 3 shows the plane distribution of two large-energy microseismic events obtained at the 13200 fully mechanized caving face. It can be seen that the two high-energy microseismic events are located near the F16 fault, at the same time, the continuous activity of the F16 fault will lead to further redistribution of stress in its vicinity. Therefore, in specific parts of the F16 fault, a high local tectonic stress concentration area is often formed, and the concentration of tectonic stress leads to the accumulation of elastic deformation potential. When underground engineering activities approach this area, the original stress balance state of coal and rock mass is destroyed due to the superposition of tectonic stress and mining stress. When the accumulated elastic energy is greater than the consumed energy, the energy will be released, and the released energy will be released. The energy will lead to the occurrence of dynamic disasters such as mine rock burst.

The two groups of high-energy microseismic events at 9:59 am on February 10, 2021 and at 3:41 pm on March 6, 2021 are as follows Table 1.

Table 1
large energy microseismic events

Serial number	date	time	X	Y	Z	energy	face/mining area/coal seam
1	2021-02-10	09:59:45	71281	2661	49	7.1E + 6	13200/east area/2–3
2	2021-03-06	15:41:59	71384	2742	31	1.2E + 6	13200/east area/2–3

It can be seen from the above table that the microseismic energy monitoring value at 3:14 pm on March 6 was 3.40E + 03. With the passage of time, the energy gradually increased, reaching a peak value at 3:41 pm, the monitoring value was 1.20E + 06, and then the monitoring value decreased; The energy followed the same variation pattern in the microseismic monitoring on February 10.

In the 13200 working face, The mine earthquake energy release of coal mining is mainly concentrated in these two days. With the progress of mining activities, mine earthquakes frequent at all times. The mine vibration frequency during production is significantly higher than that during shift shifts, and the energy release is also higher than that during maintenance. There is a hysteresis in stress release, the frequency of mine shock and energy release will not stop immediately after the mining stop in the mining area, and there is a certain time for stress stability adjustment.

Because the fault destroys the continuity of the coal layer, the evolutionary law of mining stress becomes very complicated. It is easy to form stress concentration areas in the faulty area. When the mining face is close to fault, it is easy to release the accumulated elastic energy. The advance bearing pressure increases with the continuous advancement of the working face. The superimposition with the bearing pressure formed by the fault slip causes the rockburst. The process of elastic energy accumulation is the incubation stage of rock burst, which belongs to static load; The slip and instability of the upper and lower walls of the fault near the working face is equivalent to applying a shock wave source to the surrounding rock of the fault, and the energy is transmitted to the stressed coal body to apply dynamic load. The dynamic shock is generated by the slip shearing of the fault, and the stress level after the superposition of the instantaneous dynamic stress increment and the static stress in the coal pillar when the energy is released and transferred to the coal pillar exceeds the ultimate strength of the coal body. lead to damage to coal rock mass.

The elastic deformation of coal and rock mass and the accumulation of energy are a steady state process, while the process of coal rock mass destruction and energy release is an unstable process. Due to the action of excavation and unloading, the original stress of the coal body changes rapidly from the three-direction stress state to the two-direction stress state to the one-direction stress state.

The elastic deformation energy accumulated in the original rock stress field of the surrounding rock of the roadway is calculated by the generalized Hooke's law:

$$E_J = \frac{\sigma_1^2 + \sigma_2 2 + \sigma_3^2 - 2u\left(\sigma_1\sigma_2 + \sigma_2\sigma_3 + \sigma_1\sigma_3\right)}{2E}$$

1

Where: σ is the stress

E is the elastic modulus

According to the theory of rock burst start. The generation process of rock burst is divided into three stages. The sequence is shock initiation - shock energy transfer - shock ground pressure manifestation. The energy criterion for shock start is:

$$E_J + E_D - E_C > 0$$

Among them, E_C is the energy required for buckling failure under the unidirectional stress state of the coal body, and E_D is the energy transferred to the equilibrium region after attenuation.

With the advancement of the 13200 working face, the influence range of the advanced bearing pressure extends forward,When encountering the bearing pressure formed by the fault slip, a superposition effect is formed to form a large energy concentration in the superposition area, When the energy criterion E_J + E_D-E_C > 0 for the occurrence of fault rock burst is satisfied, the induced fault activation will cause rock burst failure. This also verifies that the relevant research shows that the hard top and bottom sandstone easily accumulates a large amount of elastic deformation energy. The coal-rock mass is affected by the roof and the floor, and the dynamic shock is released during the breaking of the hard roof and the slip of the fault, so that the coal-rock mass in the critical state has a violent rock burst accident.

After monitoring the 13200 working face near the F16 fault for a period of three months (January 1, 2021 to March 8, 2021), the microseismic time series characteristics are shown in Fig. 4, where the maximum energy is 7.1×106J, It is greater than the critical energy 104 for the occurrence of rock burst, so rock burst is very likely to occur at this stage.

4. Monitoring Of F16 Fault

4.1 monitoring purpose

In order to ensure the safe production of the working face, microseismic monitoring technology is applied to predict the rock burst in the coal mining near-fault area. Quantitatively reflect the impact hazard status and hazard level of coal mining adjacent fault areas from time sequence and space, explain the mine geological conditions and mining activities in the mining area affect the activity law of the fault, the mining intensity and mining layout of different mining areas and the coal mine geological area. Changes also affect the regular changes of faults. Underground monitoring of the F16 fault was carried out to grasp the changes of displacement and stress of the F16 fault during the mining process, and to provide

basic data for the prevention and mitigation of ground pressure in the 13200 working face of Gengcun Coal Mine and the southern connecting face.

Based on microseismic monitoring, the law of fault activation was analyzed, and it was found that most of the microseismic events occurred near each fault. Now the specific appearance is basically consistent with this precursory phenomenon. By continuously summarizing and summarizing the fault law, the rock burst in the adjacent fault area of coal mining can be accurately predicted.

4.2 monitoring scheme

(1) In the first survey area, construct a monitoring hole to the Triassic hard roof, and quantitatively measure the variation of tension and displacement at the coal-rock interface. Figure 5 shows the construction model of the first surveying area of the 13200 working face.

(2) 4 test drill holes are arranged along the strike in the first survey area, marked as A, B, C, and D respectively. A and B measuring holes are arranged in the same form, which are used for the determination of the active tension of the fault; The C and D measuring holes are used to measure the active displacement of the fault. The C measuring hole "test group" passes through the coal-rock interface and is fixed in the rock layer; the D measuring hole "test group" is fixed in the coal seam near the coal-rock interface., the test group is required to be fixed with a sealing bag at a distance of 6 m from the bottom of the hole. The layout of the measuring holes is shown in Fig. 6.

(3) The distance from the roadway to the coal-rock interface is 20 m, the elevation angle of the measuring hole is 36°, as shown in Fig. 7, and the ruler is arranged;

(4) Set baffles and sealing bags at a position 6 m away from the hole bottom. To prevent liquid leakage, wrap the outer end of the sealing tape with a layer of cotton cloth; Pour grout into the baffle to fix the "test group";

(5) After the installation of the tensile test group is completed, curing is not less than 72 hours. Use the puller to test whether the anchor cable meets the requirements, and install the anchor cable lock; An anchor cable dynamometer is installed at the outer end of the anchor cable to measure the tension change after the coal-rock interface moves.

(6) In the displacement test measuring hole, after the grouting is completed, the outermost end of the measuring pipe is marked with a scale to measure the displacement change after the coal-rock interface moves.

(7) The overall construction effect of tensile force monitoring is shown in Fig. 8, and the overall construction effect of displacement monitoring is shown in Fig. 9.

Force measuring point A starts monitoring at 10:00 on January 25, 2021, with a reading of 6.30 kN, By the end of monitoring at 10:26 on April 1, 2021, the reading was 65.30 kN. When dynamometer A is damaged, this point is 10.2 m away from the working surface at the end of monitoring. Tensile force

measurement point B started monitoring at 10:00 on January 25, 2021, with a reading of 5.80 kN, and ended at 12:00 on March 21, 2021, with a reading of 105.96 kN. When dynamometer B is damaged, this point is 21.2 m away from the working surface at the end of monitoring.

Displacement measuring points C and D start counting from January 26, 2021, and end on March 21, 2021; Work face ranging was conducted on January 26, February 29, March 2, and March 5, 2021. On March 21, 2021, due to the maintenance of the roadway of the 13200 working face, the displacement test point measuring tube was damaged.

4.3 result analysis

(1) Monitoring tension and stress data analysis.

The tensile force monitoring period from point A is from January 26 to April 5, 2021. The tensile force value increased from the initial value of 6.3 kN to 65.3 kN, an increase of 59 kN, which was 10.4 times higher than the initial value. The overall growth trend was stable. During the period, the working face 37 m advanced.

The tensile force monitoring period from point B is from January 26 to March 8, 2021. The tensile force value increased from the initial value of 5.8 kN to 105.96 kN, an increase of 100.16 kN, an increase of 17.3 times compared with the initial value, and the growth rate was large. During the period, the working face advanced 27 m.

Comparing the readings of the two stress measuring points, the tensile force growth of measuring point A is relatively stable, the amplitude is small, and the growth rate is small. The tensile force of measuring point B increases incoherently and intermittently, but the growth rate is large, and the tensile force increases rapidly. There is a difference in the increase and change trend of the tensile force value between the measuring point A and the measuring point B, which is caused by the difference in the hole depth of the measuring hole and the uneven distribution of lithology. The relationship between monitoring point tension and working face distance is shown in Fig. 10.

The conversion between the tension value and the stress value of the monitoring point, according to the "Coal Industry Standard of the People's Republic of China" (MT/T 942–2005), the conversion relationship between the tension and stress of the anchor cable is shown in formula (4 − 1):

$$R_0 = \eta_0 . n . S_n . R_m \quad (4-1)$$

In the formula: R0 is the maximum force of the mine anchor cable, N; η0 is the efficiency coefficient of the machine anchor (take 0.95); n is the number of steel strands; Sn is the reference cross-sectional area of a single steel strand, mm2; Rm is the steel Stranded tensile strength, MPa.

Calculated from formula (4 − 1):

Anchor cable stress (Rm) = 2.86 × anchor cable tension (R0),

Or expressed as: anchor cable tension (R0) = 0.35 × anchor cable stress (Rm), the variation of anchor cable tension and stress with the working surface distance is shown in Fig. 11, see Table 2.

Table 2
Variation of anchor cable tension and stress with working face distance

Measuring point No.	Tension variation /kN	Stress variation /MPa	Working face distance /m	Monitoring time
A	6.30—65.30	18.00—186.76	55.20—10.20	1.25—4.5
B	5.80—105.96	16.59—303.05	45.00—20.00	1.25—3.8

It can be seen from Fig. 11 that with the advancement of the working face, the distance between the working face and the measuring point A and measuring point B gradually becomes smaller, and the tensile force shows an obvious linear increase. The fitting function obtained by data fitting is as follows:

Measuring point A:

$$F_A = 1.2421x_A + 72.73,\ R^2 = 0.9776\ (4-2)$$

Measuring point B:

$$F_B = 4.7256x_B + 195.96,\ R^2 = 0.9819\ (4-3)$$

It can be seen from Fig. 12 that with the advancement of the working face, the distance between the working face and the measuring point A and measuring point B gradually decreases, and the stress shows a significant linear increase. The fitting function obtained by data fitting is as follows:

$$P_A = 3.4992x_A + 206.58,\ R^2 = 0.9743\ (4-4)$$

Measuring point B:

$$P_B = 11.12x_B + 491.52,\ R^2 = 0.93\ (4-5)$$

According to formula (4 − 2) and formula (4 − 3), every time the working face is advanced by 1 m, the tension of the anchor cable at the measuring point A increases by 1.24 kN, and the stress of the anchor cable increases by 3.50 MPa.

It can be obtained from equations (4–4) and (4–5) that for every 1 m advance of the working face, the anchor cable tension at measuring point B increases by 4.73 kN, and the anchor cable stress increases by 11.12 MPa.

(2) Monitoring displacement and delamination data analysis

The displacement monitoring period is from January 26 to March 7, 2021, during which the working face has advanced 27 m.The anchoring end of the measuring pipe at measuring point C is in the rock

formation of the upper wall of F16, and the anchoring end of the measuring pipe at measuring point D is in the coal seam of the lower wall of F16. The variation of the displacement of the measuring point with the distance of the working surface is shown in Table 3.

Table 3
Variation of measuring point displacement with working face distance

Measuring point No.	Initial reading /mm	Final reading /mm	Working face distance /m	Monitoring time
C	1625	1395	45.00–19.60	1.26–3.7
D	1230	1100	52.20–26.80	1.26–3.7

During the monitoring period, the measurement tube reading of measuring point C changed from 1625 mm to 1395 mm, and the displacement was 230 mm, and the measurement tube reading of measuring point D changed from 1230 mm to 1100 mm, and the displacement was 130 mm. The displacement change of the upper and lower disks of F16 during the monitoring period is calculated to be 100 mm. That is, under the influence of mining, the F16 fault produced a separation of 100 mm during the monitoring period. With the advancement of the working face, the distance between the working face and the displacement measuring points C and D gradually decreases, and the displacement increases linearly. During the monitoring period, the displacement variation of the upper and lower plates of F16 (amount of separation of layers) was 100 mm, and when the working face was 40 m away from the monitoring point, the displacement of the monitoring point increased significantly; When the working face is advanced by 1 m, the monitoring displacement increases by 5.3–8.5 mm. It shows that the mining of the working face caused the activity of the F16 fault, the displacement of the measuring point increased, and the upper and lower walls of the F16 were separated. The relationship between the displacement of the monitoring point and the distance between the monitoring point and the working surface is shown in Fig. 12.

In order to find out the impact of high-energy microseismic events on the displacement and stress measurement points, the high-energy microseismic events monitored near the 13200 working face of the Gengcun Coal Mine around February 9 and March 7 were checked. The details are shown on the Table4–5–6–7.

Table 4
microseismic data (February 9)

Date	Time	Energy /J
2021/2/9	8:18:29	3000
2021/2/9	8:31:20	140000
2021/2/9	8:46:36	3000
2021/2/9	9:33:45	7100000
2021/2/9	10:22:03	1500

Table 5
microseismic data (March 7)

Date	Time	Energy /J
2021/3/7	8:33:24	1600
2021/3/7	8:41:55	55000
2021/3/7	8:41:59	1200000
2021/3/7	8:52:37	740
2021/3/7	9:28:35	280
2021/3/7	9:07:57	5400

Table 6
stress changes of measuring points a and B on February 9

Measuring point No	Monitoring time	Tension variation /kN	Stress variation /MPa
A	8:00–10:00	3.58	10.239
B	10:00–12:00	3.32	9.495

Table 7
stress changes of measuring points a and B on March 7

Measuring point No	Monitoring time	Tension variation /kN	Stress variation /MPa
A	8:00–10:00	3.61	10.325
B	8:00–10:000	3.42	9.781

It can be seen from the tensile force monitoring data that the tensile force data of measuring point A was 14.35 KN at 8:00 am on February 9th, and the tensile force data was 17.93 KN at 10:00 am, and the tensile force increased by 3.58 KN within two hours. According to the formula :

Anchor cable stress (RM) = 2.86 × Anchor cable tension (R0) (4–6)

It can be seen that the stress has changed by 2.86 × 3.58 = 10.2388 MPa. The measuring point B was at 10:00 am on February 9, the tensile force data was 21.85 KN, and at 12:00 am, the tensile force data was 25.17 KN, and the tensile force increased within two hours. 3.32 KN, the stress change is 2.86 × 3.32 = 9.4952 MPa.

Measuring point A was at 8:00 am on March 7th, the tensile force data was 29.79 KN, and at 10:00 am, the tensile force data was 33.4 KN, an increase of 3.61 KN in two hours, According to formula (4–6), it can be known that the stress has changed by 2.86 × 3.61 = 10.3246 MPa, The tensile force data of

measuring point B at 8:00 am on March 7 is 101.07 KN, and the tensile force data of 10:00 am is 104.49 KN, an increase of 3.42 KN in two hours, and the stress change is 2.86 × 3.42 = 9.7812 MPa.

The displacement change curve is shown in Fig. 13. From January 26 to February 3, the displacement increased smoothly, with a total increase of 5 mm. rom February 9 to February 11, the displacement increased sharply, increased by 25 mm, and the displacement increased by 100%. The sharp increase in the displacement in a short period of time indicated that the energy in the coal rock increased instantaneously, From February 9 to March 7, the displacement increments flattened again, increasing by 5 mm, and from March 7 to March 9, the displacement increased sharply again, increasing by 16 mm, from March 9 By March 21, the displacement increments continued to be gentle, with increments of 5 mm, and on March 21, the monitoring equipment was damaged and data recording stopped.

In the figure above, the displacement increased slowly from January 26 to February 3, indicating that the elastic potential energy in coal and rock at this time was in the accumulation stage, which belonged to the gestation process of rock burst. From February 9 to 2. There were two sharp increases on March 11 and from March 7 to March 9, the increase was 25 mm and 16 mm, and the increase was 100%. The sharp increase in the displacement in a short period of time represents an instantaneous increase in the energy inside the coal and rock mass, indicating that the occurrence of a large-energy microseismic event has imposed a shock wave source on the surrounding rock, and the energy is transmitted to the stressed coal mass to apply a load, and the released energy is transmitted to the coal pillar. The instantaneous stress increment becomes larger, and the performance reflected on the sensor is that the amplitude of the tensile force value of the measuring point increases, that is, a high-energy microseism occurs.

(3) Verification of coal-rock power system

The occurrence of rockburst arises from the fact that the difference between the energy released by the failure of coal and rock mass and the energy consumed reaches or exceeds a certain critical value. Different energy differences lead to different degrees of dynamic manifestation of rock burst, and energy differences depend on the relative spatial relationship between mining engineering and coal-rock dynamic system. In order to better describe the relationship between the coal-rock dynamic system and the rockburst appearance, a “relationship model between the coal-rock dynamic system and the rockburst” was constructed, as shown in Fig. 14.

According to the characteristics of energy accumulation degree and influence range, the coal rock power system can be divided into "power core area", "failure area", "damage area" and "influence area". The three areas of " power core area", " failure area" and "damage area" will have the danger of rock bursts of different degrees and forms of damage. According to the intensity of rockburst, rock bursts can be divided into coal cannon (no impact), dumping or extrusion (weak impact), rock burst (moderate impact) and severe rock burst (strong impact), etc. levels. When the excavation project enters the "influenced area", the power is mainly manifested in the form of "coal cannon"; when the excavation project enters the " damage area ", the power is mainly manifested in the form of "extrusion and dumping"; when the excavation project enters the " failure area ", the dynamic force appears as "bursting ground pressure";

When the excavation project enters the " power core area", "strong shock ground pressure" will be generated. Therefore, it is of great significance to study the structure of the coal-rock dynamic system and determine the calculation method of each regional scale for the targeted prevention and control of mine rock burst.

According to the dynamic analysis software of coal-rock dynamic system, when the elastic modulus is 7.64×108 Pa and the energy is 7.1×106 J, the dynamic core radius can be calculated as 3.38 m, according to the area formula πR2 The output area is 35.87m2. When the elastic modulus is 7.64×108 Pa and the energy is 1.2×106 J, the dynamic core radius can be calculated to be 1.87 m, and the area can be calculated to be 10.98 m2 according to the area formula (4–7).The values of parameters in coal rock dynamic system are shown in Table 8.

$S = \pi R^2$ (4–7)

S: the area of the circle in the dynamic nucleus

R: the radius of the circle in the dynamic nucleus

Table 8
values of parameters in coal rock power system

Serial number	Elastic modulus /Pa	Energy /J	Radius /m	Area /m^2
1	7.64×10^8	7.1×10^6	3.38	35.87
2	7.64×10^8	1.2×10^6	1.87	10.98

A mathematical relationship is established between the stress of coal and rock mass, the displacement monitored to move, and the area of the "dynamic core area" in the coal-rock dynamic system. After integration, the energy released by coal and rock mass can be obtained [30,31], and the following formula is obtained:

$E=\iiint \sigma \Delta x \, s$ (4-8)

σ: Stress of coal and rock mass

Δx: Displacement under stress

s: Area of "power core" in coal rock power system

E: Energy in coal and rock mass

Substituting the data in the above table into formula (4–8), it can be concluded that the stress at point A on February 9 is 10.24 MPa, the displacement increment is 25 mm, the dynamic core area is 35.87 m2, and the energy is 9.18×106 J. On February 9, the stress at point B was 9.5 MPa, the displacement

increment was 25 mm, the dynamic core area was 35.87 m2, and the energy was 8.52×106 J. On March 7, the stress at point A was 10.33 MPa, the displacement increment was 16 mm, the dynamic core area was 10.98 m2, and the energy was 1.82×106 J. On March 7, the stress at point B was 9.78 MPa, the displacement increment was 16 mm, the dynamic core area was 10.98 m2, and the energy was 1.72×106 J.A. The energy values monitored at two points B are shown in Table 9.

Table 9
energy values monitored at points a and B

time	σ/MPa	Δx/mm	s/m2	E/J
point a February 9,	10.24	25	35.87	9.18×106
point b February 9,	9.50	25	35.87	8.52×106
Point a, March 7	10.33	16	10.98	1.82×106
Point b, March 7	9.78	16	10.98	1.72×106

Through the monitoring results of stress, displacement and area, we can know the energy changes of the two monitoring points A and B on February 9 and March 7, and then verify with the energy value in the "coal-rock dynamic system". are nearly equal, so the calculated energy conforms to the energy law of the "coal-rock dynamic system", From this, it can be concluded that the "Coal Rock Dynamic System Analysis" software can verify the influence of stress and displacement on energy.

5. Conclusion

(1) Yima Coalfield is a triangular fault block-Mianchi fault block and adjacent faults composed of the translational fault on the bank in the northeast, the Koumenshan-Potou fault in the northwest, the Huishan fault and the Nanpingquan fault and the F16 fault in the southern boundary. After a strong tectonic compression, a complex thrust nappe structural system was formed, which is the geological structural background condition for the rockburst in the Yima mining area.

(2) The drop of the F16 fault near the 13 mining area of Gengcun Coal Mine is 350–380 m, and it is concluded that the width of the F16 fault influence zone is 7000–7600 m. Under the combined action of mining stress and fault stress, the activity of the F16 fault increases and occurs The possibility of rock burst further increases.

(3) The significant mining impact area is located 40 m in front of the working face. The maximum tensile force of the force-measuring cable is 105.96 kN, the maximum stress of the force-measuring cable is 303.05 MPa, and the maximum monitoring displacement is 230 mm. The upper and lower walls of the F16 fault have a separation of 100 mm. It shows that the mining of the working face has an important

influence on the activity of the F16 fault. Under the action of the F16 fault nappe, the stress and displacement increase, the energy is released, and the danger of rock burst is easy to occur.

(4) Microseismic activities are closely related to mine production activities. The occurrence of fault slip instability and rock burst induced by mining action can be predicted and forecasted in advance. Be sure to provide reliable help.

(5) The mining disturbance causes changes in the stress and displacement of the coal and rock mass, which in trn causes a large change in the energy. The energy is in line with the energy change value of the "dynamic core area" in the dynamic system of the coal and rock mass. Through the reverse verification of the dynamic system, it is concluded that the stress is caused by the fault., displacement and energy changes, high-energy microseismic events occurred in the "dynamic core region".

Declarations

Data Availability

The data used to support the findings of this study are available from the corresponding author upon request.

Conflicts of Interest

The authors declare that they have no conflicts of interest.

References

1. Gou Panfeng, Hu Youguang Study on roof rock movement characteristics of mining roadway near fault [J] Journal of mining and safety engineering, 2006 (03): 285–288
2. Meng Zhaoping, Peng Suping, Feng Yu, et al Influence of fault structure on ground pressure and roof stability of mining face [J]
3. Sun Yuzhen Study on thrust nappe structure and its control on Rockburst in Yima coalfield [J] Coal mine modernization, 2012 (04): 35–36
4. Luo Hao, Li Zhonghua, Wang Aiwen, et al Study on evolution law of stress field near fault in deep mining [J] Journal of coal, 2014,39 (02): 322–327
5. Zhang Ningbo, Zhao Shankun, Zhao Yang, et al Study on unloading instability mechanism of thrust fault [J] Journal of coal, 2020,45 (05): 1671–1680
6. Tian Fujun Analysis and prevention practice of rock burst in Yima coalfield [J] Coal mining, 2010,15 (04): 100–102
7. Kang Hongpu, Wu Zhigang, Gao Fuqiang, et al Influence of underground geological structure on in-situ stress distribution in coal mine [J] Journal of rock mechanics and engineering, 2012,31 (S1): 2674–2680

8. Zhang Yanbo, Kang Zhiqiang, Jiang Guohu, et al Numerical simulation of roadway fault rockburst in Laohutai mine [J] Mining research and development, 2008 (02): 21–22
9. Cao Minghui, Liu fan, Wang Tongxu Numerical simulation of fault activation process and coal pillar instability mechanism [J] Journal of Shandong University of science and Technology (NATURAL SCIENCE EDITION), 2020,39 (02): 61–68
10. Jateng, Reid Numerical simulation analysis of the influence of coal and rock mechanical parameters on fault type rockburst [J] China coal, 2017,43 (03): 58–61
11. Dou Yunfeng, Li Ye, Zhu Liyuan Numerical simulation of coal seam rockburst risk at fault [J] Light industry science and technology, 2015,31 (09): 87–88
12. Dai linchao Research status and trend of fault rockburst in China [J] Zhongzhou coal, 2015 (10): 11–13
13. Zeng Linsheng, song Guihong, Yao Tianbo Study on the influence of fault on the risk of rockburst in coal mine [J] Geotechnical foundation, 2020,34 (04): 502–506
14. Pan Yishan, Wang Laigui, Zhang Mengtao, Xu bingye Theoretical and experimental study on the occurrence of fault rockburst [J] Journal of rock mechanics and engineering, 1998 (06): 642–649
15. Wang Su Na, sun Xiao Yan F_ (16) Coal control mode of thrust fault and its influence on coal seam occurrence [J] Coal technology, 2015,34 (12): 161–164
16. Liu Jinhai, Jiang Fuxing, Zhu Sitao Study on evolution law and application of dynamic and static abutment pressure in LONGWALL STOPE [J] Journal of rock mechanics and engineering, 2015,34 (09): 1815–1827
17. Li Zhonghua, Bao Siyuan, Yin wanlei, et al Study on disturbance activation conditions of giant thrust fault mining [J] Journal of mining and safety engineering, 2019,36 (04): 762–767
18. Peng Suping, Meng Zhaoping, Li Yulin Similar simulation test study on the influence of faults on roof stability [J] Coalfield geology and exploration, 2001 (03): 1–4
19. Jiang Yaodong, pan Yishan, Jiang Fuxing, et al Mechanism and prevention of rockburst in coal mining in China [J] Journal of coal, 2014,39 (02): 205–213
20. Jiang Yaodong, Zhao Yixin Research status of coal mine rockburst in China: mechanism, early warning and control [J] Journal of rock mechanics and engineering, 2015,34 (11): 2188–2204
21. Dong Sensen, Liu Weijian, Zhang Chenxi, et al Coupling study of oblique normal fault activation based on microseismic monitoring and numerical simulation [J] Journal of Zhongyuan Institute of technology, 2020,31 (05): 39–45
22. Luo H, Li Z H, Wang A W, et al. Study on the evolution law of stress field when approaching fault in deep mining[J]. Journal of China Coal Society, 2014, 39(2): 322–327.
23. Jiao Z, Yuan Q, Zou P, et al. Case study of the characteristics and mechanism of rock burst near fault in yima coalfield, China[J]. Shock and Vibration, 2021, 2021.
24. Jiao Z, Wang L, Zhang M, et al. Numerical Simulation of Mining-Induced Stress Evolution and Fault Slip Behavior in Deep Mining[J]. Advances in Materials Science and Engineering, 2021, 2021.

25. Wang H, Shi R, Deng D, et al. Characteristic of stress evolution on fault surface and coal bursts mechanism during the extraction of longwall face in Yima mining area, China[J]. Journal of Structural Geology, 2020, 136: 104071.
26. Wang H, Xue S, Shi R, et al. Investigation of fault displacement evolution during extraction in longwall panel in an underground coal mine[J]. Rock Mechanics and Rock Engineering, 2020, 53(4): 1809–1826.
27. Zhao Yangsheng, Feng Zengchao, Wan Zhijun Minimum energy principle for dynamic failure of rock mass [J] Journal of rock mechanics and engineering, 2003,22 (11): 1781–1783.
28. Rong Hai, Zhang Hongwei, Liang Bing, Han Jun, Wang Yadi Instability mechanism of coal rock dynamic system [J] Journal of coal, 2017,42 (07): 1663–1671.
29. Liu Hongquan, Yang Zhenhua, LAN Tianwei, Rong Hai Application of regional scale calculation method of coal rock dynamic system in rockburst risk assessment [J] Contemporary chemical research, 2021, (16): 79–81.
30. Rong Hai, Yu Shiqi, Zhang Hongwei, Liang Bing, Han Jun, LAN Tianwei, Yang Zhenhua Determination of critical depth of rockburst mine based on energy of coal rock dynamic system [J] Journal of coal, 2021,46 (04): 1263–1270.
31. Ronghai Study on geological dynamic conditions of rockburst and coal rock dynamic system in Wudong coal mine [D] Fuxin: Liaoning University of engineering and technology, 2016:89–102.

Figures

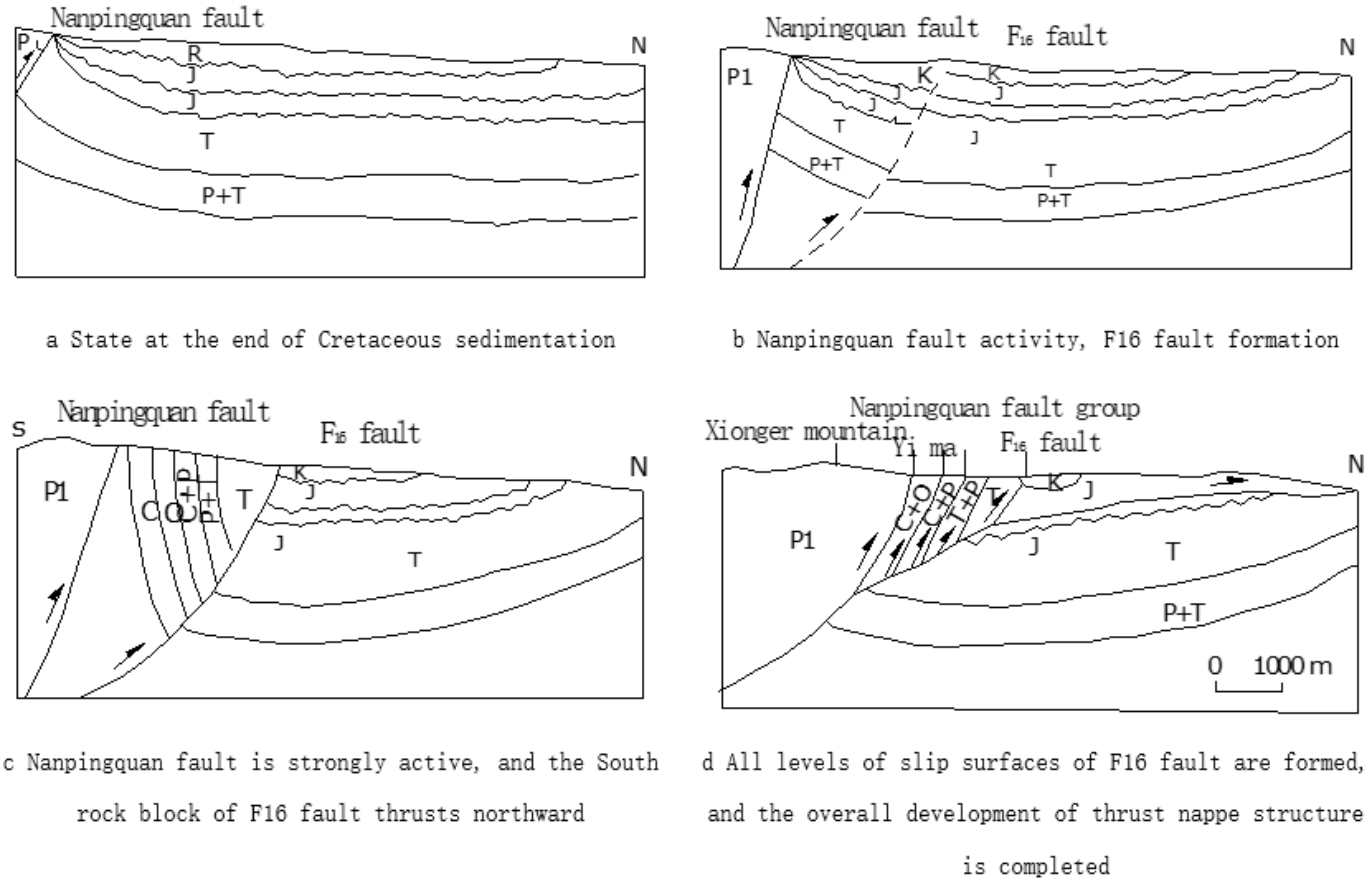

a State at the end of Cretaceous sedimentation

b Nanpingquan fault activity, F16 fault formation

c Nanpingquan fault is strongly active, and the South rock block of F16 fault thrusts northward

d All levels of slip surfaces of F16 fault are formed, and the overall development of thrust nappe structure is completed

Figure 1

evolution diagram of Yima thrust nappe structural belt

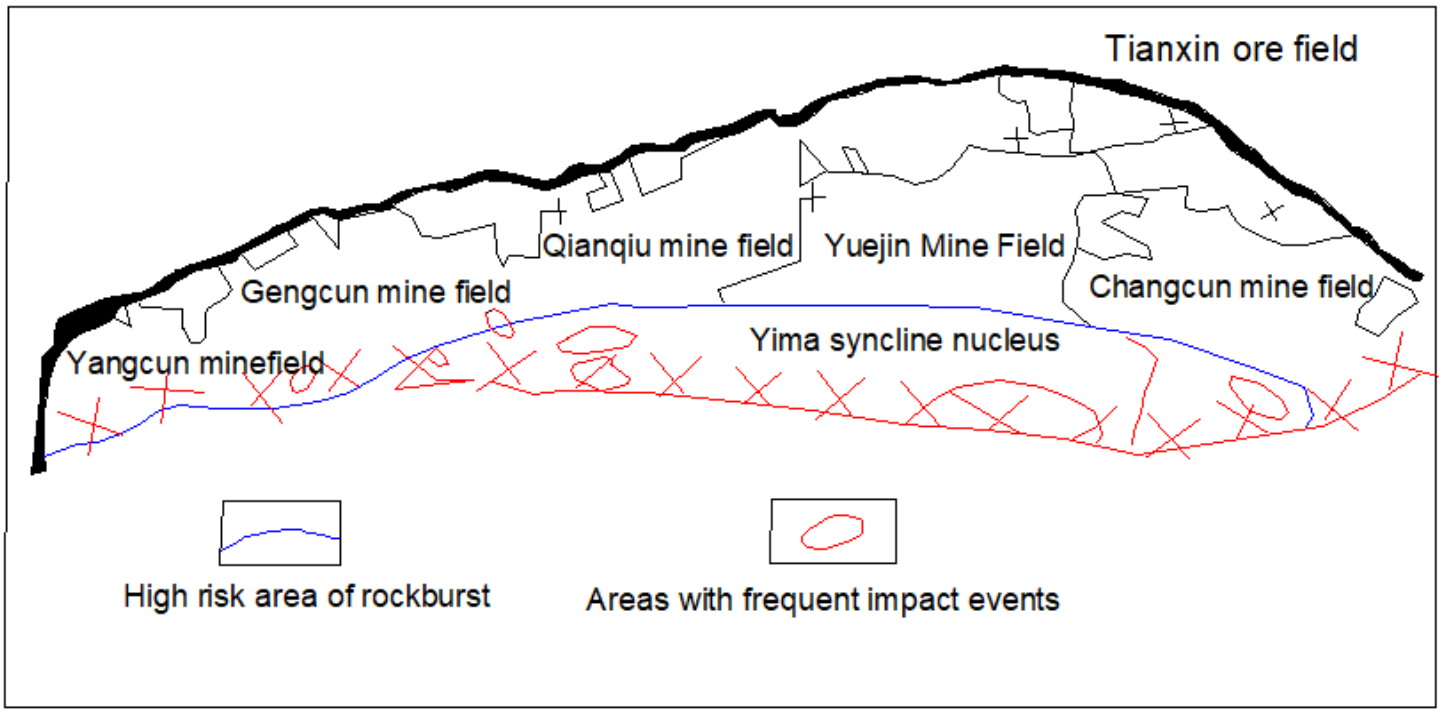

Figure 2

distribution of rockburst dangerous areas in Yima coalfield

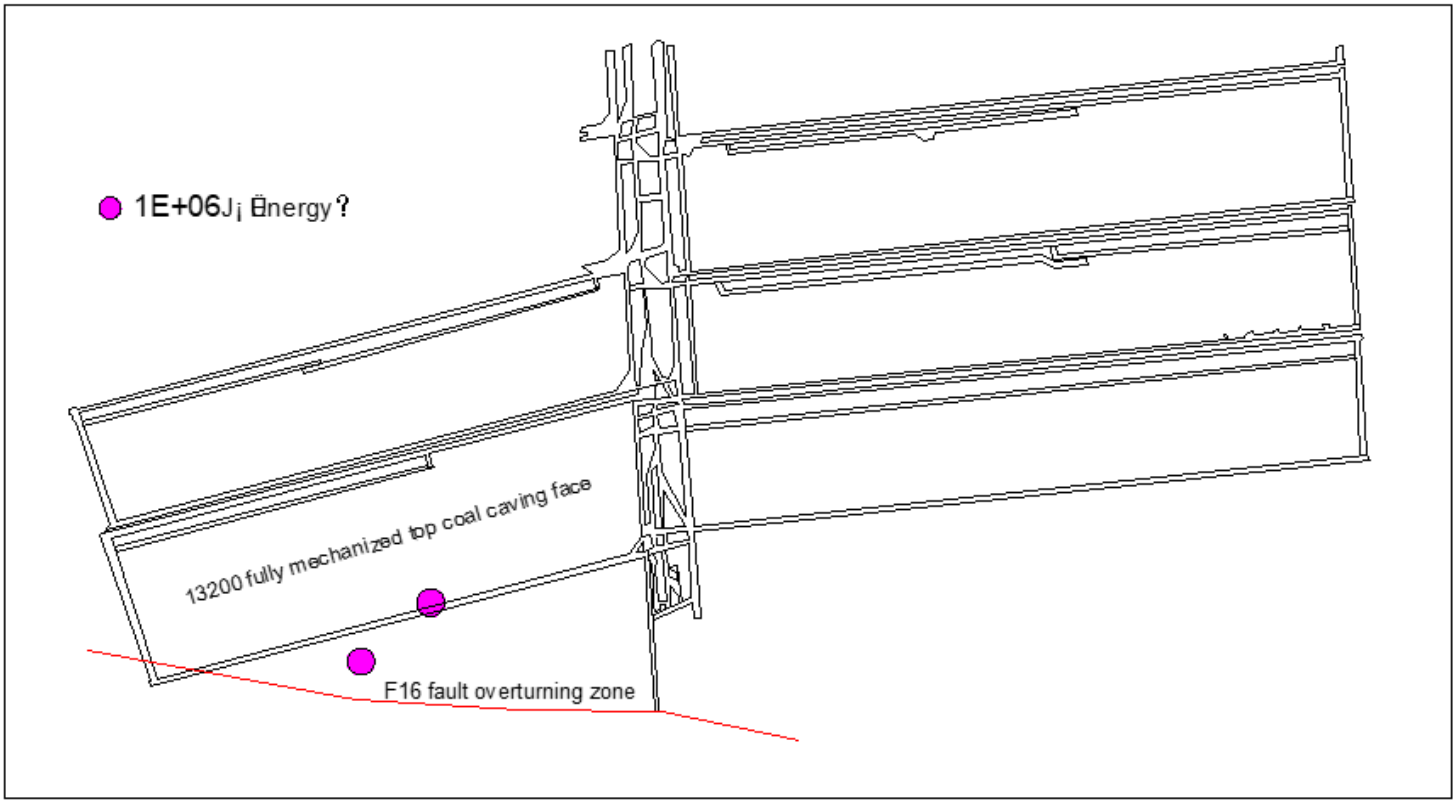

Figure 3

plane distribution of large energy microseismic events

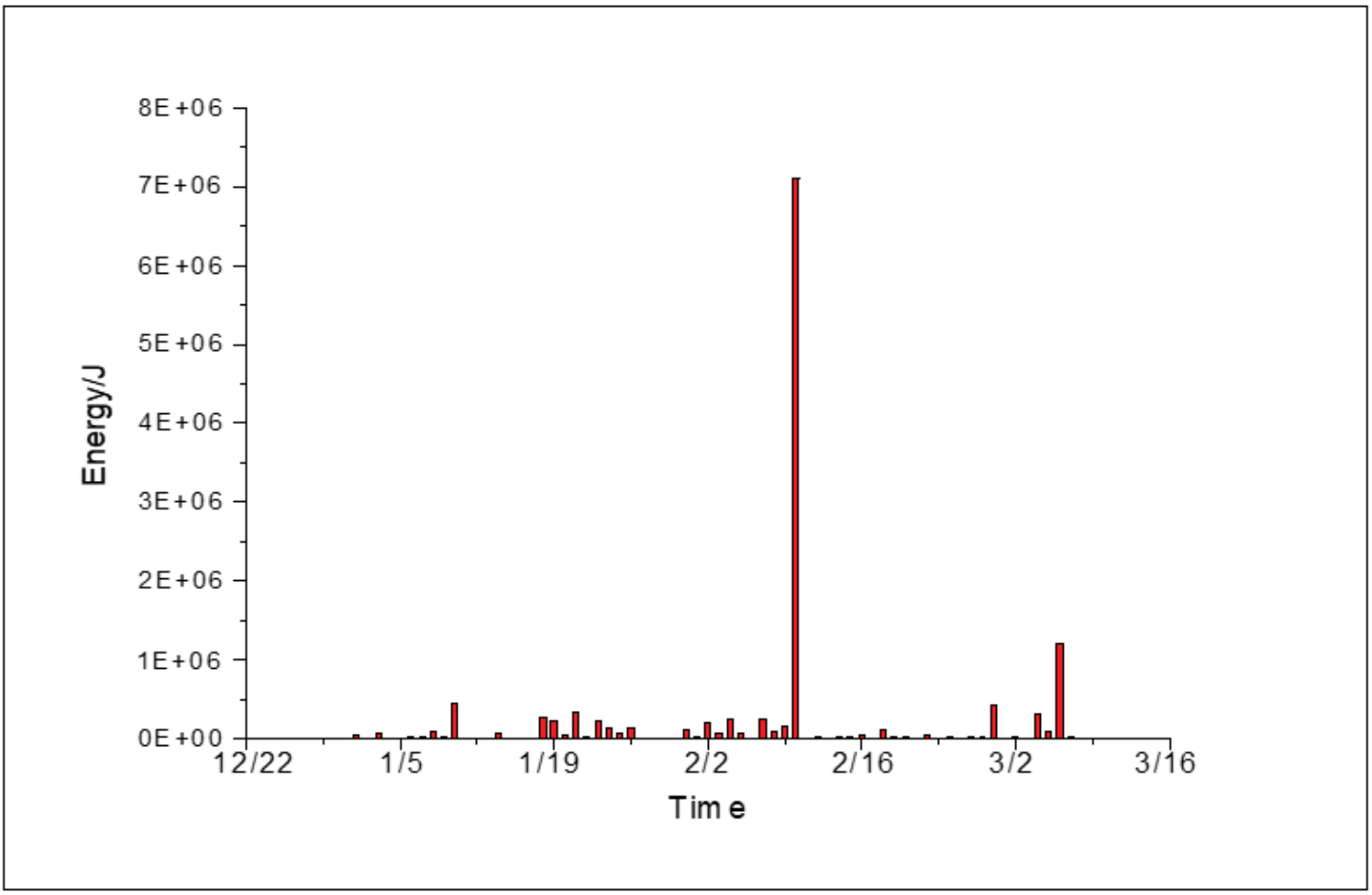

Figure 4

microseismic sequence characteristics

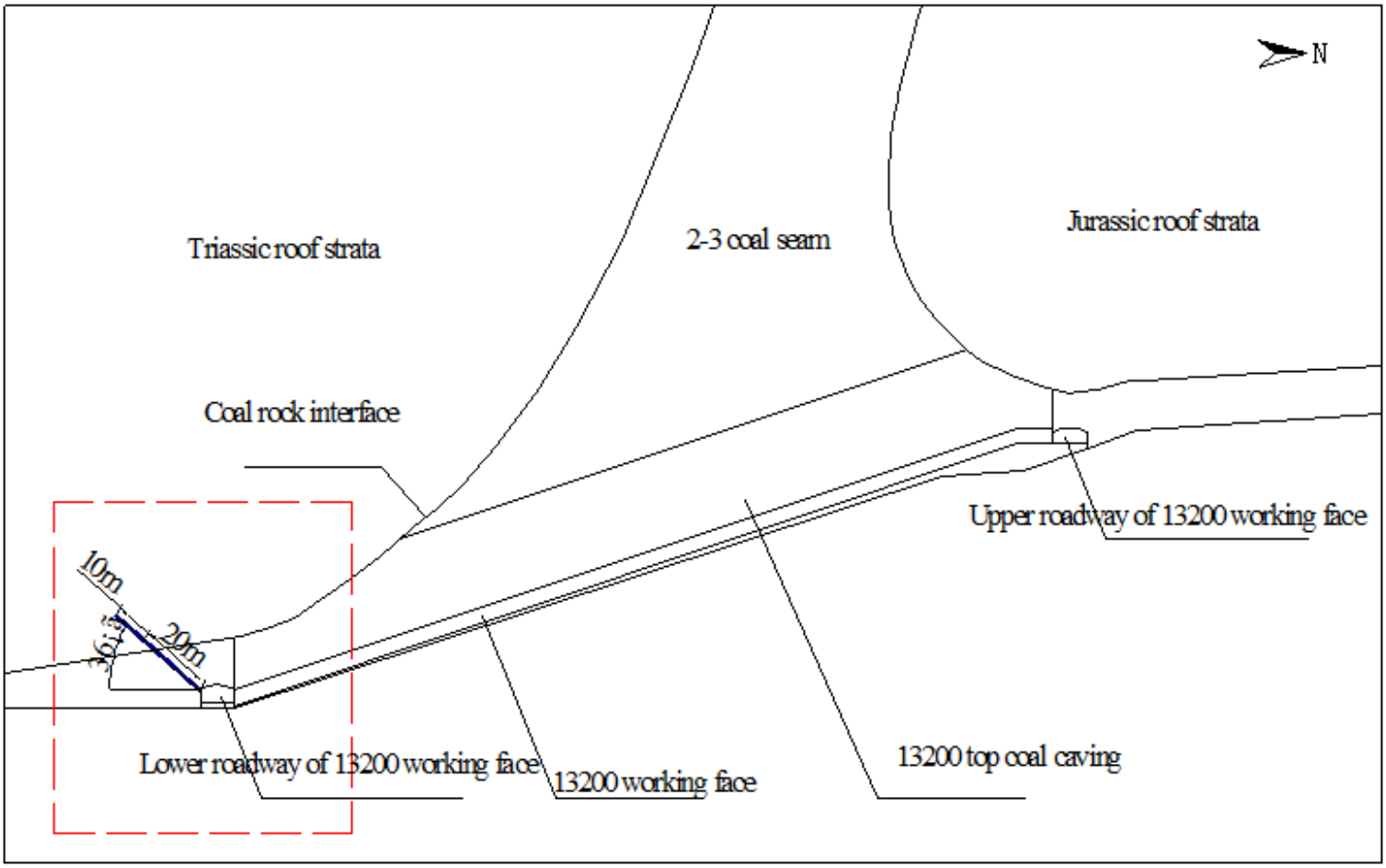

Figure 5

construction model of measuring hole in the first measuring area of 13200 working face

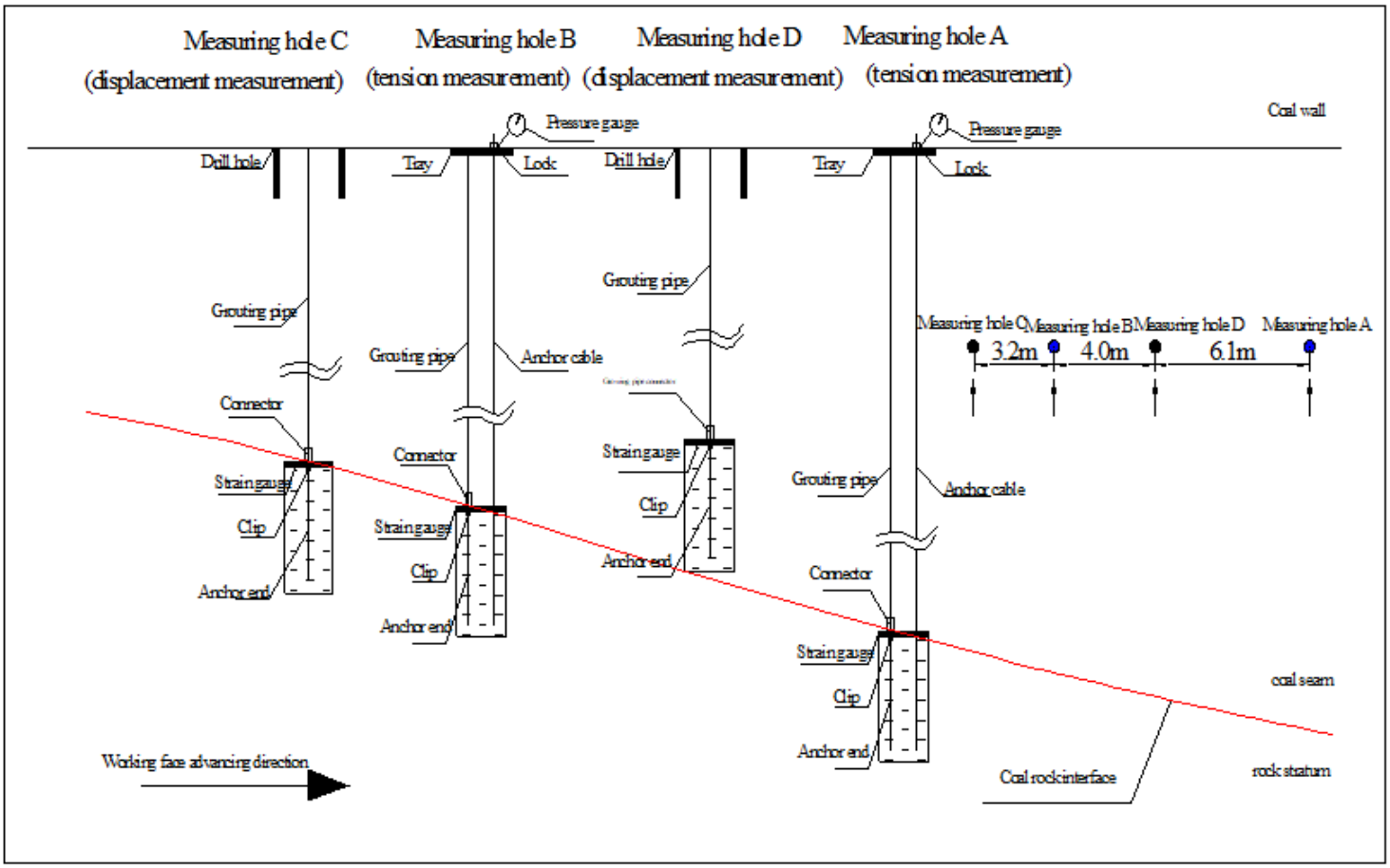

Figure 6

layout plan of survey holes in the first survey area of 13200 working face

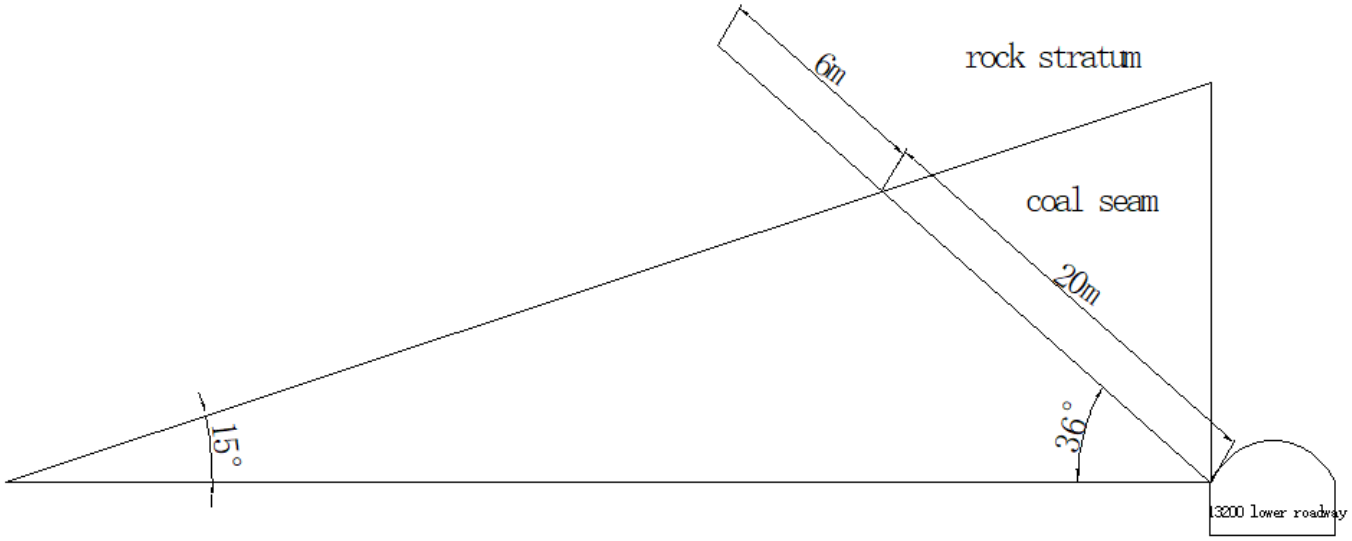

Figure 7

sectional view of measuring hole layout at measuring point 1

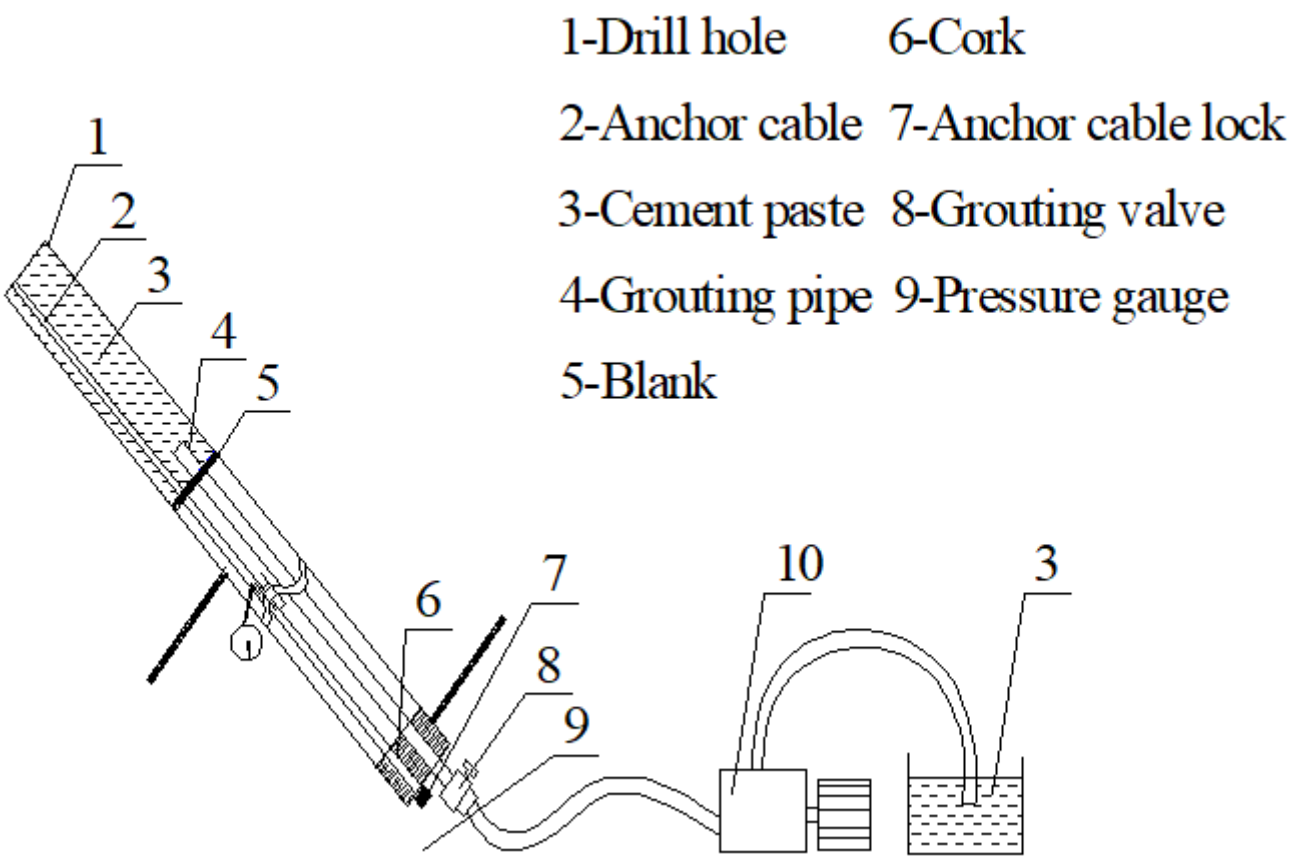

Figure 8

overall construction effect of tension monitoring

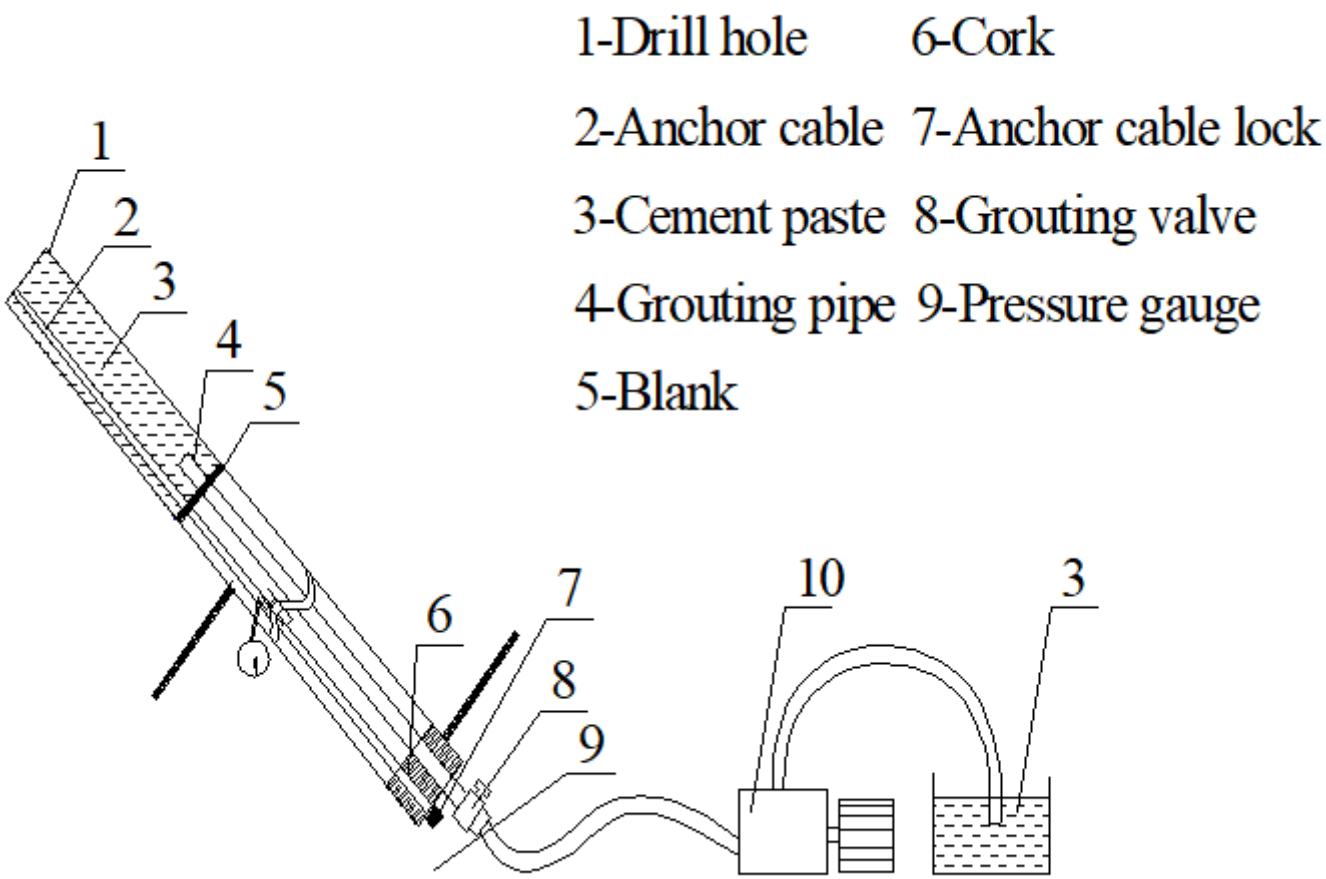

Figure 9

overall construction effect of displacement monitoring

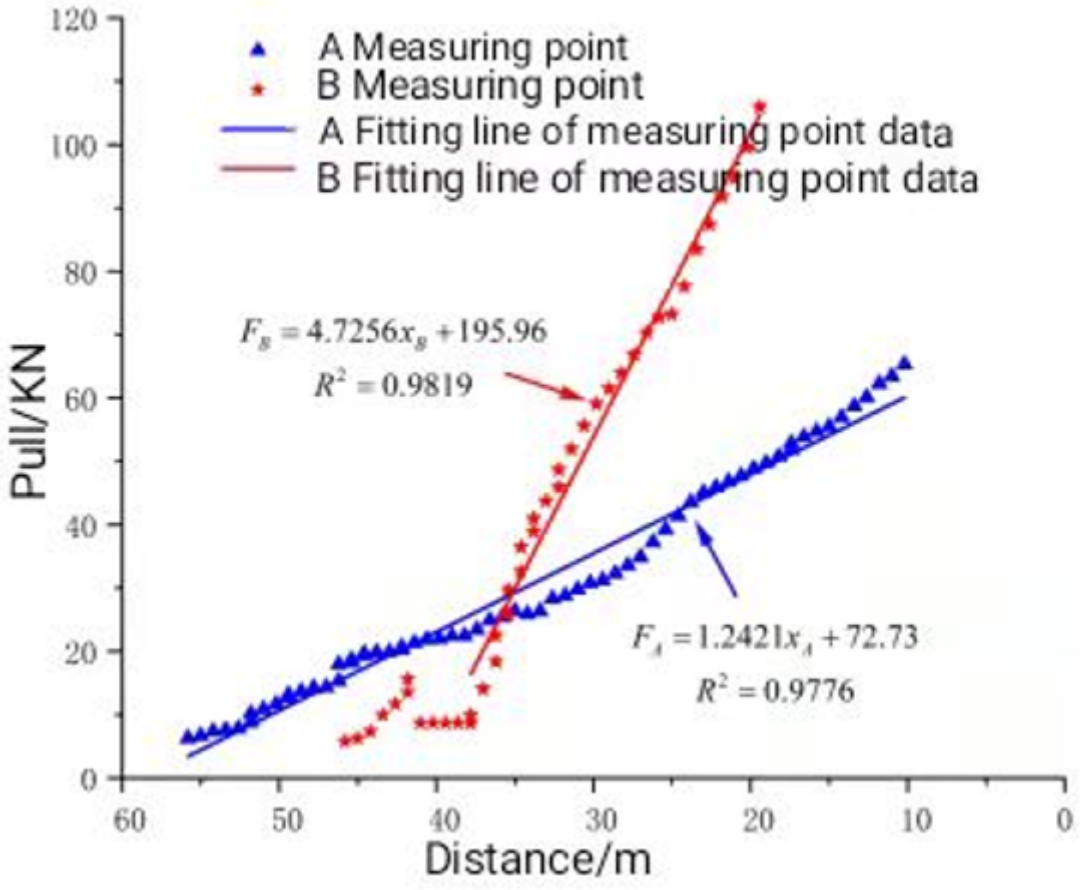

Figure 10

relationship between tension at monitoring points and working face distance

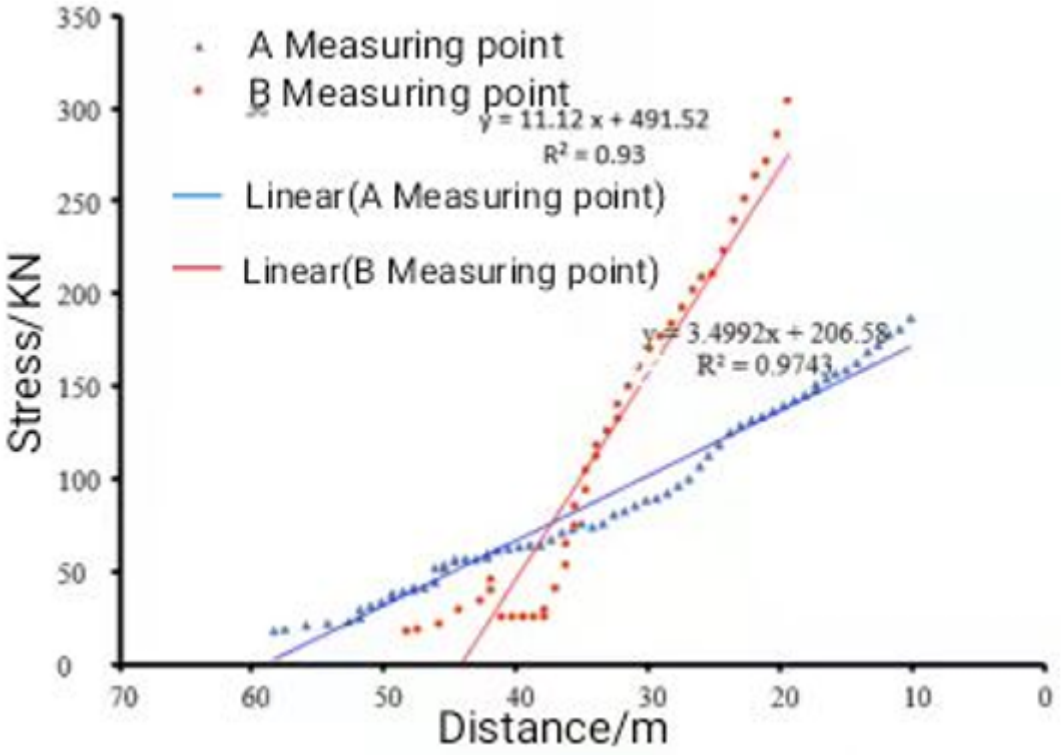

Figure 11

relationship between stress at monitoring points and working face distance

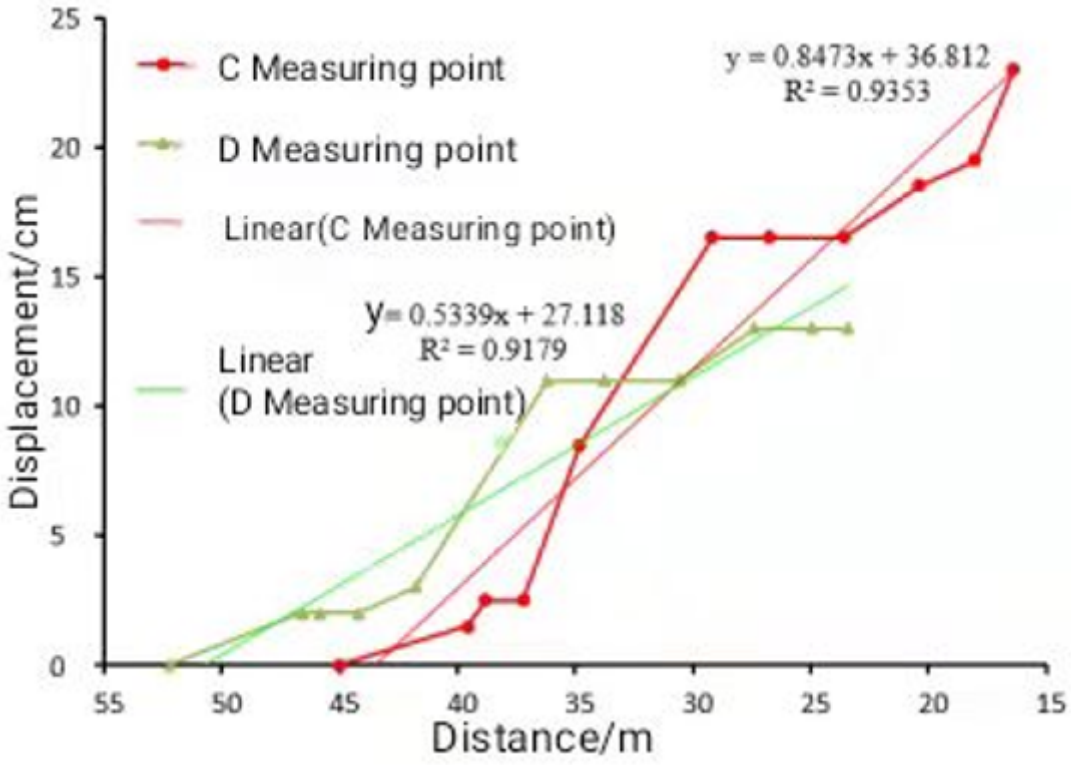

Figure 12

relationship between displacement of monitoring point and distance from measuring point to working face

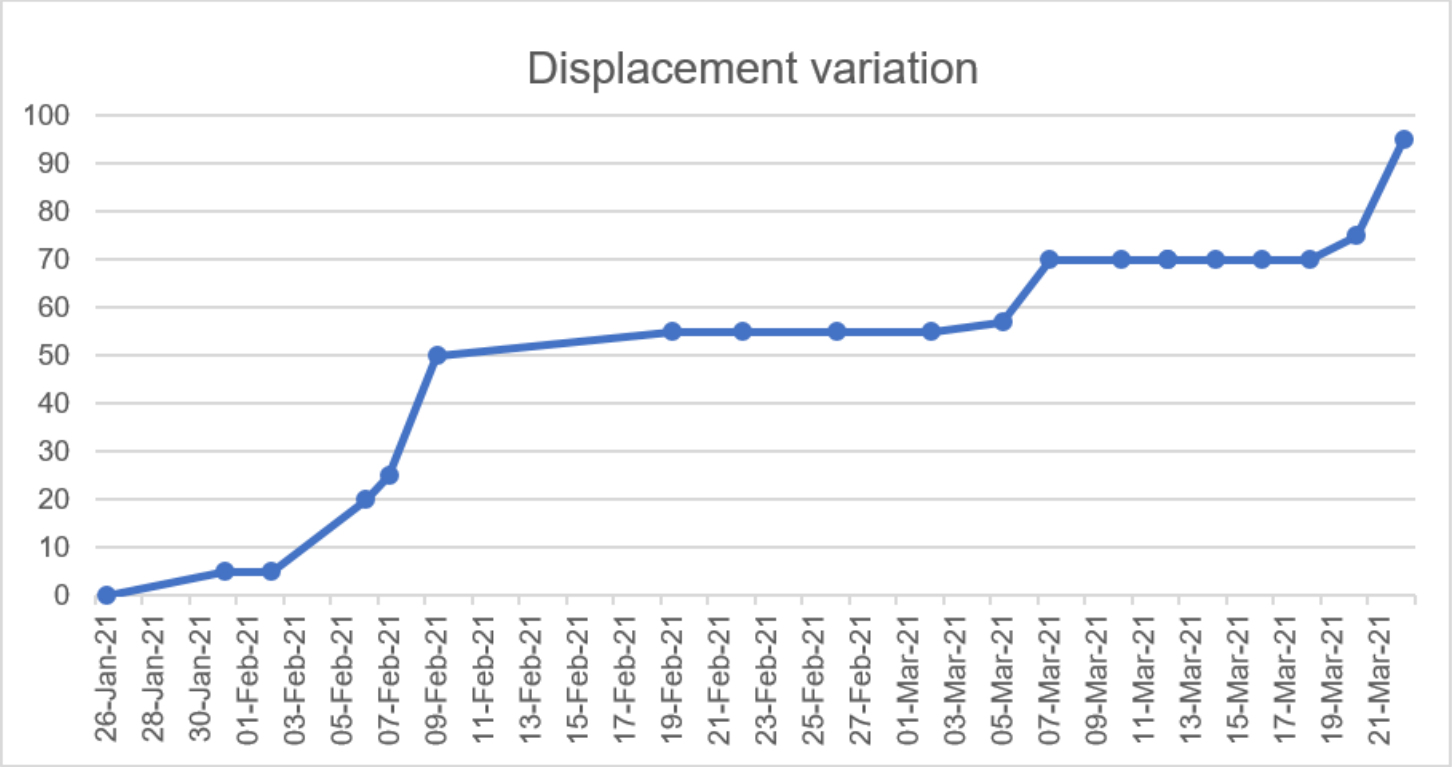

Figure 13

displacement change curve of monitoring points

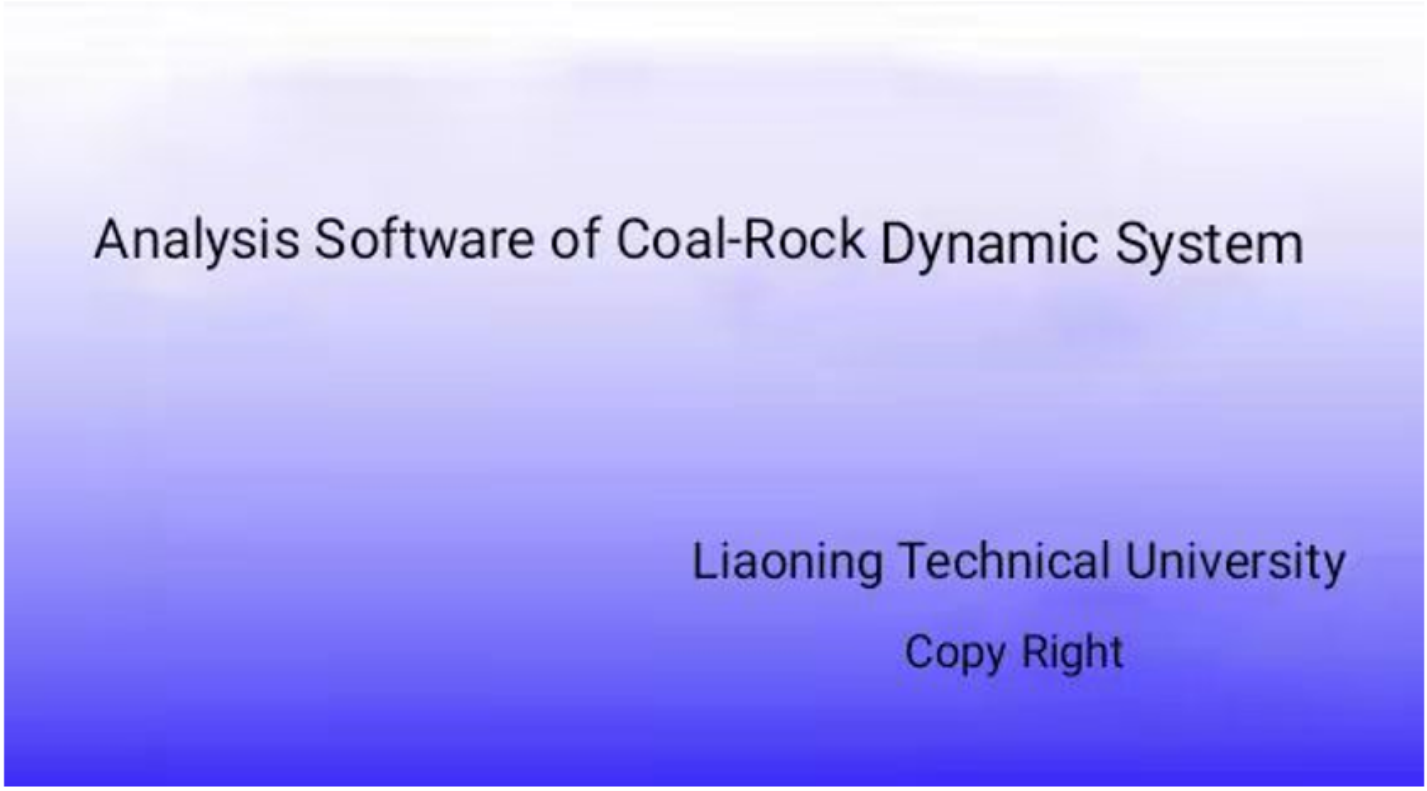

Figure 14

dynamic analysis software of coal rock power system